

Plasma-Resonance Scattering from Small Sodium Particles Formed in a Flowing Gas Stream*

C. J. Duthler, S. E. Johnson, and H. P. Broida

Department of Physics, University of California, Santa Barbara, California 93106

(Received 22 March 1971)

We have observed plasma-resonance scattering of light from sodium particles of less than 100 Å diam produced in a flowing inert gas. The scattered light near resonance was at least 90% linearly polarized and had a nearly Lorentzian peak near 320 nm with a full width at half-maximum of 60 nm. Depending on experimental conditions, the observed plasma-resonance peak varied from 310 to 330 nm, with slightly varying widths. The wavelengths of the experimentally observed resonance were about 15% less than theoretically expected. A second maximum in scattered intensity was observed at 220 nm.

Plasma-resonance absorption of light in the near-ultraviolet spectral region due to small metallic particles has been studied by several experimenters. Such absorption has been studied primarily with small silver¹⁻⁴ and gold²⁻⁵ particles and with colloidal sodium particles⁶ in NaCl. Particles studied in previous experiments have been formed by various methods, such as on a substrate by nucleation from a thin film³⁻⁵ or as colloidal particles^{1,2,6} in solids or liquids.

We have studied the scattering of white light from sodium particles of less than 100 Å diam formed in a flowing inert gas, and have made the first observation of plasma-resonance scattering from particles. The resonance is observed as a maximum in the scattered-light intensity near 320 nm, corresponding to the previously observed absorption maximum. Particles in a gas stream have the advantage of eliminating impurities and the need for optical corrections due to a background solid or liquid.

The apparatus for generating small sodium particles is shown schematically in Fig. 1.^{7,8} In this apparatus, an alumina crucible containing metallic sodium is located within a heated alumina chimney. An inert carrier gas such as nitrogen or helium flows upward through the chimney and carries the sodium to the light-scattering cell. Under certain experimental conditions, particles in the gas stream can be visually observed under white-light illumination as a pale blue plume in the light-scattering cell, directly above the heater assembly.

At heater temperatures of about 700 K and carrier gas flow rates of about 1 cm³/sec at STP, the particles in the gas above the heater are observed to form spontaneously. At elevated temperatures or flow rates, particles do not form, and fluorescence from atomic and diatomic sodium is observed.⁸ Under these conditions, it is found that particles are formed when a second

gas stream carrying water vapor is added above the chimney through the tube shown in Fig. 1. The observed particulate light-scattering characteristics are independent of the two methods of particle formation within the present experimental accuracy. Although direct measurements of sodium particle sizes and shapes have not yet been made, other metallic particles produced in this laboratory were measured with an electron microscope to be typically 30-Å-diam spheres.

The particles are illuminated by mirror-focused white light from a 450-W xenon arc lamp. Scattered light from the particles is collected at 90° from the incident light beam and spectrally analyzed with a 0.8-m grating monochromator of Czerny-Turner design. This monochromator has a wavelength resolution of 2 nm for the 2-mm slits used in the present experiments. The dispersed light from the monochromator is detected

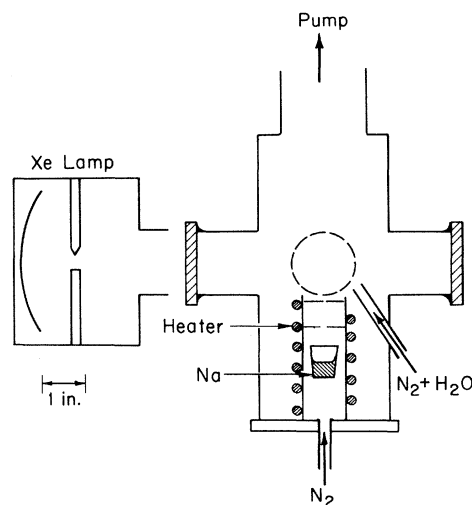


FIG. 1. Schematic drawing of the particle-generating apparatus, light source, and light-scattering cell. Particles are created when an inert gas flows upward through the heated alumina chimney. Water vapor is sometimes added to aid in particle formation.

with either of two photomultiplier tubes. A photomultiplier with a tri-alkali photocathode (EMR Model No. 541E) is used in the spectral region from 250 to 450 nm and a cesium telluride photocathode (EMR Model No. 541F) is used in the overlapping spectral region from 200 to 350 nm.

Relative scattered-light intensity as a function of wave length is determined by taking the ratio of the observed scattered-light intensity from the particles to the spectral-intensity characteristics of the lamp and optical system. The intensity characteristics of the lamp and optical system were obtained by measuring light scattered from a diffuse white reflector of BaSO_4 powder⁹ mounted in the experimental cell in place of the particles. Since scattered light from particles is observed to be linearly polarized, the optical system was tested for polarization effects in the spectral region from 270 to 500 nm. Small corrections were made to the data for two grating anomalies, which would have caused a 30% emphasis in horizontally polarized light at 340 and 380 nm.¹⁰

The data shown in Fig. 2 are typical of our measurements of the relative scattered-light intensity as a function of wavelength from 200 to 450 nm. The three curves shown in Fig. 2 were obtained at a constant pressure of 30 Torr, a constant heater power, and with the carrier gas flow equal to 1.1, 2.1, and 2.7 cm^3/sec at STP in curves A, B, and C, respectively. Curve A was obtained from particles that were formed without adding water. Curves B and C were obtained with a slight amount of water vapor added above the heater assembly to aid in particle formation.

The scattered light is characterized by being at least 90% vertically polarized, as measured from 270 to 450 nm, and by having an approximately Lorentzian peak near 320 nm due to plasma resonance.

We notice from Fig. 2 that as the carrier gas flow is increased, a second peak in intensity at about 220 nm becomes more pronounced. These three curves were drawn by first smoothly joining the separately measured spectral regions and then normalizing the entire curve so that the long-wavelength intensity maximum had unit value.

The plasma-resonance peak is observed to shift from 330 nm in curve A to 310 nm in curve C as the carrier gas flow is increased. Under experimental conditions of curve B, a full width at half-maximum of 60 nm is observed while curves A and C have a slightly greater width.

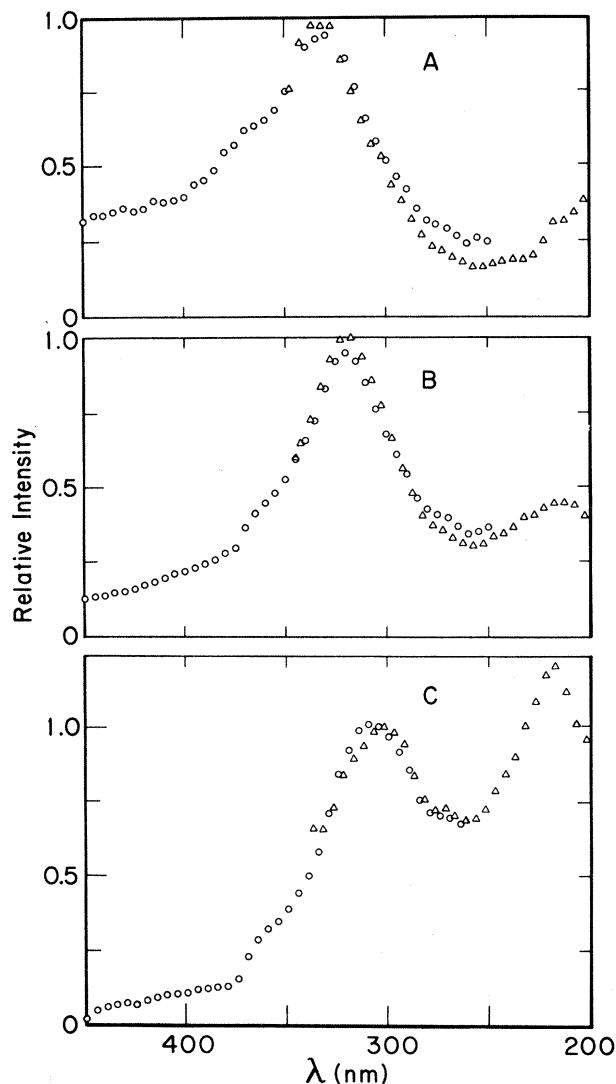


FIG. 2. Relative scattered-light intensity as a function of wavelength for inert gas flow rates of 1.1, 2.1, and 2.7 cm^3/sec at STP in curves A, B, and C, respectively. Circles and triangles were obtained with two different photomultiplier tubes. The relative intensities of the two regions were joined smoothly and normalized to unity at the long-wavelength maximum.

These scattering curves are qualitatively similar to absorption curves obtained by Doyle⁶ and others.¹⁻⁵

Plasma-resonance scattering by small metallic particles can be simply described by considering the interaction between the incident light and the conduction electrons. For particles less than 100 Å diam and visible light, we need only consider Rayleigh scattering, which is the small-particle limit of Mie scattering.¹¹ For Rayleigh scattering from a spherical particle, the power scattered per unit solid angle at 90° from an inci-

dent unpolarized light beam is linearly polarized and has the magnitude¹²

$$Q = \omega^4 p^2 / 8\pi c^3, \quad (1)$$

where ω is the light frequency, c is the velocity of light, and p is the magnitude of the oscillating induced dipole moment of the particle.

Following Yamaguchi,³ the induced dipole of the metallic particle can be simply calculated from free-electron theory. For a spherical metallic particle having N free electrons of mass m per unit volume, the magnitude squared of the oscillating dipole moment is given by

$$p^2 = \frac{(Ne^2 E_0 V / m)^2}{(\omega^2 - \omega_p^2 / 3)^2 + (\omega / \tau)^2}, \quad (2)$$

where

$$\omega_p^2 = 4\pi Ne^2 / m. \quad (3)$$

Here V is the volume of the particle, E_0 is the component of the applied electric field normal to the scattering plane, ω_p is the bulk plasma frequency, and τ is the relaxation time. The factor $\frac{1}{3}$ multiplying ω_p^2 in Eq. (2) comes from the depolarization factor for a sphere used in the calculation of the induced field within the particle.

Doremus² considers the size-dependent relaxation time τ in Eq. (2) to be determined primarily by scattering of conduction electrons from the particle surface. Kawabata and Kubo¹³ present a quantum-mechanical treatment of the plasma resonance in which they interpret the broadening of the resonance to be due to energy transfer from the plasma mode to quasiparticle excitations.

Combining Eqs. (1) and (2), we obtain the following expression for the scattered-light intensity as a function of wavelength:

$$Q = \frac{(Ne^2 E_0 V / m)^2}{8\pi c^3} \frac{\omega^4}{(\omega^2 - \omega_p^2 / 3)^2 + (\omega / \tau)^2}. \quad (4)$$

This function has a maximum at the frequency

$$\omega_R^2 = \frac{\omega_p^2 / 3}{1 - 3/2 \omega_p^2 \tau^2}. \quad (5)$$

The full width at half-maximum, $\Delta\lambda$, of the measured wavelength is related to the relaxation time τ by $1/\omega_R \tau \approx \Delta\lambda/\lambda_R$. Hence to lowest order in $\Delta\lambda/\lambda_p$, we obtain $3/\omega_p^2 \tau^2 \approx (\Delta\lambda)^2/3\lambda_p^2$. Substituting this into the denominator of Eq. (5), the resonance wavelength is found to be

$$\lambda_R^2 = 3\lambda_p^2 \left[1 - \frac{1}{6} (\Delta\lambda/\lambda_p)^2 \right]. \quad (6)$$

Sutherland, Arakawa, and Hamm,¹⁴ in their Ta-

ble II, give a summary of experimental bulk plasma energies. Using their value of $\hbar\omega_p = 5.69$ eV and our observed width, $\Delta\lambda = 60$ nm, we expect the plasma resonance emission in a small spherical sodium particle to occur at 376 nm.

Our measurements agree qualitatively with this simple classical treatment. Using either the theory of Kawabata and Kubo or the classical model of Doremus, the 60-nm width of the observed resonance indicates a particle size of about 50 Å, as expected. However, as can be seen from the data in Fig. 2, all the observed scattering maxima occur near 320 nm, which is 15% lower than expected. This shift is opposite to that which would be expected for impurities in the sodium. Any imagined impurity in sodium would be an electron sink, effectively decreasing the free-electron density N . As can be seen from Eq. (3), an impurity would be expected to decrease the plasma-resonance frequency, or increase the plasma-resonance wavelength. Furthermore, the observed shift in wavelength is not thought to be a result of the spherical depolarization factor. If the particles were ellipsoidal rather than spherical, the resonance curve would then be broader and the scattered light less polarized than observed.¹

The origin of the short-wavelength peak is not understood at this time. From the observed wavelength of this peak, it is possible that it is due to a bulk plasmon.¹⁴ Work is continuing on elucidating the short-wavelength peak and further refining the data.

*Work supported in part by the National Science Foundation Grant No. GP-14011.

¹D. C. Skillman and C. R. Berry, *J. Chem. Phys.* **48**, 3297 (1968).

²R. H. Doremus, *J. Chem. Phys.* **40**, 2389 (1964), and **42**, 414 (1965).

³S. Yamaguchi, *J. Phys. Soc. Jap.* **15**, 1577 (1960).

⁴R. S. Sennett and G. D. Scott, *J. Opt. Soc. Amer.* **40**, 203 (1950).

⁵W. Hampe, *Z. Phys.* **152**, 476 (1958).

⁶W. T. Doyle, *Phys. Rev.* **111**, 1067 (1958).

⁷K. Sakurai, S. E. Johnson, and H. P. Broida, *J. Chem. Phys.* **52**, 1625 (1970).

⁸S. E. Johnson, K. Sakurai, and H. P. Broida, *J. Chem. Phys.* **52**, 6441 (1970).

⁹F. Grum and G. W. Luckey, *Appl. Opt.* **7**, 2289 (1968).

¹⁰J. B. Breckinridge, *Appl. Opt.* **10**, 286 (1971).

¹¹G. Mie, *Ann. Phys. (Leipzig)* **25**, 377 (1908). See also M. Kerker, *The Scattering of Light and Other Electromagnetic Radiation* (Academic, New York,

1969).

¹²J. D. Jackson, *Classical Electrodynamics* (Wiley, New York, 1962), p. 272.¹³A. Kawabata and R. Kubo, *J. Phys. Soc. Jap.* **21**, 1765 (1966).¹⁴J. C. Sutherland, E. T. Arakawa, and R. N. Hamm,*J. Opt. Soc. Amer.* **57**, 645 (1967). For further recent optical properties of bulk sodium see also *Optical Properties and Electronic Structure of Metals and Alloys*, edited by F. Abeles (North-Holland, Amsterdam, 1966), and also R. J. Whitefield and J. J. Brady, *Phys. Rev. Lett.* **26**, 380 (1971).

Solubility of Divalent Impurities in the Alkali Halides

R. C. Bowman, Jr.

Monsanto Research Corporation, Mound Laboratory, Miamisburg, Ohio 45342*

(Received 22 March 1971)

The Born model of ionic solids was used to determine theoretical solution enthalpies of divalent impurities in the alkali halides, in the limit of infinite dilution. These calculations are based upon a generalized Mott-Littleton theory for reasonable values of the host-impurity parameters. Results are reported for Sr^{++} and Ba^{++} in NaCl, KCl, and RbCl.

Many physical properties of ionic solids are sensitive to the presence of trace amounts of aliovalent impurities. Although this is a general phenomenon, most studies¹⁻³ have been concerned with the cubic alkali halides containing small quantities of divalent impurity cations. This interest is the result of the availability of good-quality single crystals to which small concentrations of specified impurities have been added. Thus, interpretation¹ of the experimental results is greatly simplified. Since the alkali halides can be adequately described by the Born theory of ionic solids, it is possible to obtain theoretical values of defect parameters after a reasonable effort.

The solubility of an impurity ion in a crystal lattice is an important parameter. For a divalent impurity in the alkali halides, the enthalpy of solution, χ , can be readily obtained from ionic conductivity measurements in the "extrinsic" temperature region. Although lattice calculations⁴⁻⁶ based upon the Born-Mayer model have successfully predicted χ values for monovalent impurities in the alkali halides, similar calculations^{7,8} for divalent impurities have failed. According to Fumi and Tosi,⁵ the major difficulty in these later studies has been the use of experimental lattice energies for the halides of divalent cations while using theoretical parameters in the remainder of the calculation. Most divalent metal halides cannot be properly treated by the Born theory because they possess noncubic crystal structures. This problem does not arise for the monovalent impurities. In this report, theoretical χ values are reported for the solubility of Sr^{++} and Ba^{++} in NaCl, KCl, and RbCl crystals,

in the limit of infinite dilution. Also, Sr^{++} and Ba^{++} Born parameters consistent with recent alkali-halide data⁹ have been estimated for the cubic SrCl_2 and BaCl_2 salts.

The lattice-model expression for the enthalpy of solution of divalent impurities in alkali halides is

$$\chi = 2W_+ - W_1 + 2W_{LA} - W_{LB}.$$

Here, W_{LA} and W_{LB} are the lattice energies of the alkali halide and the halide of the divalent cation, respectively; W_+ is the energy required to remove an alkali ion from the pure alkali halide to a state of rest at "infinity"; and W_1 is the energy required to remove a divalent impurity ion at equilibrium on a cation lattice site to a state of rest at infinity. The lattice energies can be obtained by straightforward application of the familiar Born-Mayer model.¹⁰ Because ions around a defect relax when the defect is produced and in directions depending upon the parity of charges of the ions and the defect, calculation of the energy required to remove an ion is taken as the average of the energies at the lattice site for the initial and final configurations. The energies W_+ and W_1 can only be determined when the

Table I. Born parameters and lattice energies for SrCl_2 and BaCl_2

	r_{++} (Å)	r_-^a (Å)	ρ (Å)	b (eV)	W_L (eV)
SrCl_2	1.35	1.65	0.278	0.2004	21.876
BaCl_2	1.50	1.65	0.281	0.2110	21.853

^aRef. 9.